

# The QCD Phase Diagram at Non-zero Baryon and Isospin Chemical Potentials <sup>y</sup>

D. Toublan<sup>a</sup>, B. Klein<sup>b</sup> and J.J.M. Verbaarschot<sup>c</sup>

<sup>a</sup>Department of Physics, University of Illinois at Urbana-Champaign, Urbana, IL 61801, USA

<sup>b</sup>Institute for Theoretical Physics, University of Heidelberg, 69120 Heidelberg, Germany

<sup>c</sup>Department of Physics and Astronomy, SUNY at Stony Brook, Stony Brook, NY 11794, USA

In heavy ion collision experiments as well as in neutron stars, both baryon and isospin chemical potentials are different from zero. In particular, the regime of small isospin chemical potential is phenomenologically important. Using a random matrix model, we find that the phase diagram at non-zero temperature and baryon chemical potential is greatly altered by an arbitrarily small isospin chemical potential: There are two first order phase transitions at low temperature, two critical endpoints, and two crossovers at high temperature. As a consequence, in the region of the phase diagram explored by RHIC experiments, there are two crossovers that separate the hadronic phase from the quark-gluon plasma phase at high temperature.

## 1. INTRODUCTION

Heavy ion collision experiments are important for our understanding of the strong interaction at nonzero temperature and density. In heavy ion collision experiments, both the baryon and the isospin densities are different from zero. The time between the formation of the fireball and its freezeout is so short that only the strong interactions play a significant role and baryon number as well as isospin are conserved. Therefore, it is phenomenologically worthwhile to study the effects of a nonzero isospin chemical potential,  $\mu_I$ , on the QCD phase diagram at nonzero temperature,  $T$ , and baryon chemical potential,  $\mu_B$ . However, most studies at high temperature and nonzero density have been restricted to cases where either  $\mu_I$  or  $\mu_B$  is zero.

For  $\mu_B \neq 0$  and  $\mu_I = 0$ , the phase diagram is very rich. At low  $T$  and high  $\mu_B$ , the ground state is believed to be a color superconductor [1]. If  $T$  is increased and  $\mu_B$  is decreased, a first order phase transition separates the hadronic phase from the quark-gluon plasma phase. If  $\mu_B$  is further de-

creased, this first order critical line stops in a critical endpoint. At lower  $\mu_B$ , there is a crossover between the hadronic phase and the quark-gluon plasma phase. These results are based on different models [2,3], as well as on exploratory lattice studies at low chemical potential [4].

In the case of  $\mu_B = 0$  and  $\mu_I \neq 0$ , the fermion determinant is real and traditional lattice methods can be applied. In this case, the phase diagram is very rich as well. At low  $T$ , an increase in  $\mu_I$  above the pion mass leads to a superfluid phase with a pion condensate. At low  $T$ , the phase transition between the hadronic phase and the pion condensation phase is second order and has mean field critical exponents. If  $T$  is increased, this second order phase transition becomes first order. Therefore there is a tricritical point in the phase diagram. These results were found using both lattice simulations [5] and effective theories [6]. At high  $T$  and low  $\mu_I$ , a crossover separates the hadronic phase from the quark-gluon plasma phase. There also might be a critical endpoint and a first order phase transition at high  $T$  when  $\mu_I$  is increased [5].

We use a Random Matrix model as a schematic model for QCD to study the phase diagram at

Talk presented by D. Toublan, Lattice 2004, Fermilab  
<sup>y</sup>Work supported in part by NSF grant NSF PHY 03-04252, and by US DOE grant DE-FG-88ER 40388.

nonzero  $T$ ,  $\mu_B$ , and  $\mu_I$  [7]. This model has been previously used to study QCD at  $\mu_B \neq 0$  and  $\mu_I = 0$  [3]. We then analyze possible consequences for heavy ion collision experiments.

## 2. RANDOM MATRIX MODEL

Random matrix models were introduced in QCD to describe the correlations of low eigenvalues of the Dirac operator [8]. It was shown that for large matrices these models are equivalent to the mass term of the chiral Lagrangian that is uniquely determined by the symmetry of QCD [9]. Therefore, in the chiral limit, Random Matrix Theory provides an exact analytical description of the low-lying Dirac spectrum. The idea is to replace the matrix elements of the Dirac operator by Gaussian random variables subject only to the global symmetries of the QCD partition function. The temperature and chemical potentials enter through external fields structured according to these symmetries.

For two quark flavors of mass  $m_1$  and  $m_2$ , the partition function of our model reads

$$Z = \int \prod_{i=1}^2 dW_i \det \begin{pmatrix} m_1 & W_1 \\ W_1 & m_1 \end{pmatrix} e^{-N G^2 \text{Tr} W W^\dagger}; \quad (1)$$

where  $W_i = W + i\gamma_5$ , and  $W_i^\dagger = W^\dagger + i\gamma_5$  are  $n \times n$  matrices, with  $\gamma_5 = \text{diag}(i\mathbb{1}; -i\mathbb{1})$ . The elements of the random matrix  $W$  are complex. First, we express the determinant in (1) as a Grassmann integral. Then, we perform the Gaussian integration over  $W$ . Third, the resulting four-fermion interaction is decoupled by means of a Hubbard-Stratonovich transformation at the expense of introducing mesonic degrees of freedom. Finally we perform the Grassmann integration, and the partition function (1) can be mapped onto [7]

$$Z = \int dA \exp(-L(A; A^\dagger)); \quad (2)$$

where  $A$  is an arbitrary complex  $2 \times 2$  matrix, and

$$L = N G^2 \text{Tr}(A M^\dagger)(A^\dagger M) - \frac{n}{2} \text{Tr} \log Q^\dagger Q; \quad (3)$$

with  $M = \text{diag}(m_1; m_2)$ , and

$$Q = \begin{pmatrix} A & i\mathbb{1} + \mu_B + \mu_I I_3 \\ i\mathbb{1} + \mu_B + \mu_I I_3 & A^\dagger \end{pmatrix}; \quad (4)$$

with  $I_3 = \text{diag}(1; -1)$ . This is an exact mapping.

In the large- $n$  limit, this partition function can be evaluated by a saddle point approximation. To solve the saddle point equations, we make an Ansatz for the matrix  $A$  based on the symmetry of the partition function. Since we have two independent chemical potentials, one for each quark flavor, the chiral condensates are not necessarily equal. Furthermore, at high enough  $\mu_I$ , we expect a pion condensate. We thus assume that

$$A = \begin{pmatrix} 1 & \\ & 2 \end{pmatrix}; \quad (5)$$

In this parameterization, the chiral condensates are given by  $\langle \bar{u}u \rangle = G^2(m_1 - m_2)$ ,  $\langle \bar{d}d \rangle = G^2(m_2 - m_1)$ , and the pion condensate by  $\frac{1}{2}(\langle \bar{u}d \rangle + \langle \bar{d}u \rangle) = G^2$ . We thus get an effective potential that can be studied in the usual way.

We limit ourselves to the case  $m_1 = m_2 = m$ . We are particularly interested in the phase diagram in the  $\mu_B$ - $T$  plane at  $\mu_I$  small enough so that the superfluid phase is never reached, because it corresponds to the conditions of heavy ion collision experiments. The phase diagram in the  $\mu_B$ - $T$  plane for zero  $\mu_I$  has been studied in [3]. In the chiral limit, the chiral restoration transition extends as a second order line from the  $\mu_B = 0$  axis, changes order at a tricritical point, and intersects the  $T = 0$  axis as a line of first order transition. For nonzero quark mass, the first order transition ends in a critical point, and the second order transition becomes a crossover. Figure 1 shows the phase diagram in the  $\mu_B$ - $T$  plane at finite quark mass  $m/G = 0.1$  for zero isospin chemical potential,  $\mu_I = 0$ , and for  $\mu_I/G = 0.1$ . We observe that the first order curve splits into two first order curves that are separated by  $2\mu_I/G$ . This can be understood as follows. Below the threshold for pion condensation, the free energy separates into a sum over the two flavors. For  $\mu_I = 0$ , the chiral phase transition lines for both flavors coincide. A nonzero  $\mu_I$  breaks the flavor symmetry, and the first order transition lines for the two flavors split and shift in opposite directions. The temperature of the critical endpoints is not affected by  $\mu_I$ .

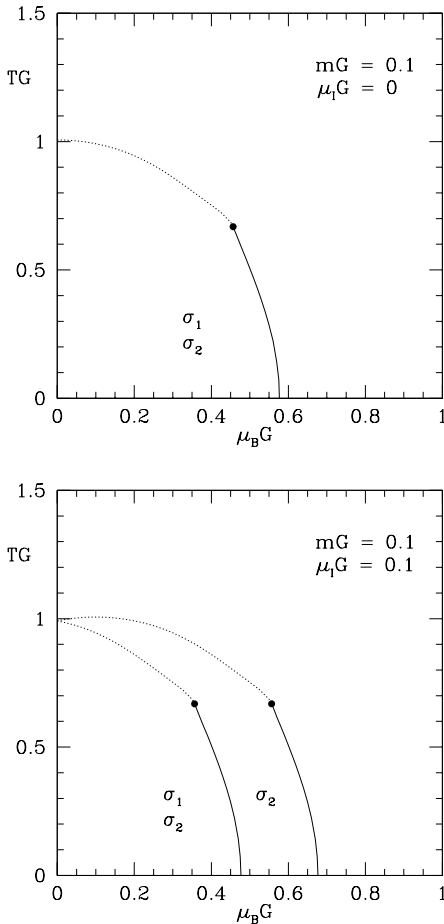


Figure 1. Phase diagram in the  $T_B$ - $T$  plane for quark mass  $m_G = 0.1$  and  $\mu_1$  as shown. First order transitions are denoted by full curves, and crossovers by dotted curves. The condensates  $\sigma_1 = \langle \bar{u}u \rangle$  and  $\sigma_2 = \langle \bar{d}d \rangle$  are omitted where  $\mu_1 = 1$ .

### 3. CONCLUSIONS

We have used a Random Matrix model for QCD at nonzero  $T$ ,  $T_B$ , and  $T_I$ . We have found that in the region of high  $T$  and small  $T_B$ , an arbitrarily small  $T_I$  greatly alters the phase diagram in the  $T_B$ - $T$  plane: There are two crossovers, two critical endpoints, and two first order phase transition lines that separate the hadronic phase from the quark gluon plasma phase [7]. This could have important consequences for heavy ion collision experiments, since they are done at  $T_B \neq 0$  and  $T_I \neq 0$ . If our Random Matrix model gives

an accurate description of the phase diagram, it might also be interesting to use different isotopes in heavy ion collision experiments in order to vary  $T_I$  at constant  $T_B$ . These results have been confirmed by other models, albeit with some constraints in one case [10]. Finally, recent lattice studies at small nonzero  $T_B$  can also be used at nonzero  $T_B$  and  $T_I$ , and will provide an important test for our results.

### REFERENCES

1. For a review see, K. Rajagopal and F. Wilczek, arXiv hep-ph/0011333.
2. A. Barducci et al, Phys. Rev. D 41, 1610 (1990); J. Berges and K. Rajagopal, Nucl. Phys. B 538, 215 (1999).
3. M. A. Halasz et al, Phys. Rev. D 58 096007 (1998).
4. Z. Fodor and S. D. Katz, JHEP 0203, 014 (2002); C. R. Allton et al, Phys. Rev. D 66, 074507 (2002); P. de Forcrand and O. Philipsen, Nucl. Phys. B 642, 290 (2002); M. D'Elia and M. P. Lombardo, Phys. Rev. D 67, 014505 (2003).
5. J. B. Kogut and D. K. Sinclair, Phys. Rev. D 66, 034505 (2002); arXiv hep-lat/0407041.
6. J. B. Kogut et al, Nucl. Phys. B 582, 477 (2000); D. T. Son and M. A. Stephanov, Phys. Rev. Lett. 86, 592 (2001); K. Splittor et al, Nucl. Phys. B 639, 524 (2002).
7. B. Klein et al, Phys. Rev. D 68, 014009 (2003).
8. E. V. Shuryak and J. J. M. Verbaarschot, Nucl. Phys. A 560, 306 (1993); J. J. M. Verbaarschot, Phys. Rev. Lett. 72, 2531 (1994).
9. J. C. Osborn et al, Nucl. Phys. B 540, 317 (1999); P. H. Damgaard et al, Nucl. Phys. B 547, 305 (1999); D. Toublan and J. J. M. Verbaarschot, Nucl. Phys. B 560, 259 (1999).
10. D. Toublan and J. B. Kogut, Phys. Lett. B 564, 212 (2003); M. Frank et al, Phys. Lett. B 562, 221 (2003); A. Barducci et al, Phys. Lett. B 564, 217 (2003).